1 **A novel pathway linking plasma membrane and chloroplasts is co-opted by**

2 **pathogens to suppress salicylic acid-dependent defences**

3 Laura Medina-Puche[1], Huang Tan[1,2], Vivek Dogra[1], Mengshi Wu[1,2], Tabata Rosas-Diaz[1,3], Liping

4 Wang[1,2], Xue Ding[1,2], Dan Zhang[1,2,4], Xing Fu[1], Chanhong Kim[1], Rosa Lozano-Duran*[1]

5 [1]Shanghai Center for Plant Stress Biology, CAS Center for Excellence in Molecular Plant Sciences,

6 Chinese Academy of Sciences, Shanghai 201602, China. [2]University of the Chinese Academy of Sciences,

7 Beijing 100049, China.

8

9 AUTHOR LIST FOOTNOTES

10 [3] Present address: Instituto de Hortofruticultura Subtropical y Mediterránea "La Mayora" (IHSM-UMA-CSIC),

11 Area de Genética, Facultad de Ciencias, Universidad de Málaga, Campus de Teatinos s/n, E-29071 Málaga,

12 Spain. [4]Present address: Department of Cell Biology, Centre for Organismal Studies Heidelberg,

13 Heidelberg University, 69120 Heidelberg, Germany.

14

15 CORRESPONDING AUTHOR

16 Rosa Lozano-Duran; email: Lozano-duran@sibs.ac.cn

17

18

19

SUMMARY

20

21   Chloroplasts are crucial players in the activation of defensive hormonal responses during plant-

22   pathogen interactions. Here, we show that a plant virus-encoded protein re-localizes from the

23   plasma membrane to chloroplasts upon triggering plant defence, interfering with the chloroplast-

24   dependent activation of anti-viral salicylic acid (SA) biosynthesis. Strikingly, we have found that

25   plant pathogens from different kingdoms seem to have convergently evolved to target chloroplasts

26   and impair SA-dependent defences following an association with membranes, which is based on

27   the co-existence of two subcellular targeting signals, an N-myristoylation site and a chloroplast

28   transit peptide. This pattern is also present in plant proteins, at least one of which conversely

29   activates SA defences from the chloroplast. Taken together, our results suggest that a pathway

30   linking plasma membrane to chloroplasts and activating defence exists in plants, and that such

31   pathway has been co-opted by plant pathogens during host-pathogen co-evolution to promote

32   virulence through suppression of SA responses.

33

KEYWORDS

34

35   Plasma membrane, chloroplast, retrograde signalling, salicylic acid, defence, geminivirus, effector,

36   pathogen, plant

37

38

2

INTRODUCTION

Beyond their role as photosynthetic organelles enabling photoautotrophy, chloroplasts are emerging as hubs in the integration of environmental stimuli and determinants of downstream responses (Chan et al., 2016, de Souza et al., 2017, Zhu, 2016, de Torres Zabala et al., 2015, Xiao et al., 2013, Zhao et al., 2016). A growing body of evidence substantiates the fundamental function of chloroplasts in orchestrating defence responses: upon perception of a biotic threat, this organelle acts as the source of calcium and reactive oxygen species (ROS) bursts and communicates with the nucleus through retrograde signalling, initiating a signalling cascade that leads to the expression of defence-related genes, including those responsible for the biosynthesis of the defense hormone salicylic acid (SA), subsequently produced in the chloroplast stroma (Serrano et al., 2016; Nomura et al., 2012). The chloroplast-nucleus communication during Pattern-Triggered Immunity (PTI) involves the so-called Calcium Sensing Receptor (CAS), a thylakoid membrane-associated protein; although the exact molecular function of CAS in unclear, this protein is required for PTI-induced transcriptional reprograming, SA biosynthesis, callose deposition, and anti-bacterial resistance (Nomura et al., 2012). How the information of pathogen attack is relayed from the cell periphery (e.g. during a bacterial infection) or possibly other subcellular compartments (e.g. during viral infections) to chloroplasts, however, remains elusive, while the molecular basis of retrograde signalling during defence responses are largely unexplored.

In agreement with a prominent role of chloroplast function in defence and in the context of the arms race between pathogens and hosts, a number of virulence factors from evolutionarily unrelated pathogens belonging to different kingdoms of life, including bacteria, viruses, fungi, and oomycetes, have been described to target this organelle (e.g. de Torres Zabala et al., 2015, Fondong et al., 2007, Rodriguez-Herva et al., 2012, Rosas-Diaz et al., 2018, Jelenska et al., 2007, Jelenska et al., 2010, Li et al., 2014, Liu et al., 2018, Park et al., 2017, Petre et al., 2016). Some plant viruses co-opt chloroplast membranes to build viral replication factories (Jin et al., 2018; Bhattacharyya and Chakraborty, 2018) but, intriguingly, plant proteins from other viruses can also be found in chloroplasts (Vaira et al., 2018; Bhattacharyya and Chakraborty, 2018; Rosas-Diaz et al., 2018; Zhan et al., 2018; Bhattacharyya et al., 2015; Liu et al., 2015). In a few cases, it has been demonstrated or suggested that chloroplast-localized viral proteins can promote viral pathogenesis (Gnanasekaran et al., 2019; Bhattacharyya et al., 2015; Krenz et al., 2010). We recently showed that the C4 protein from the geminivirus *Tomato yellow leaf curl virus* (TYLCV), a DNA virus replicating in the nucleus, contains two overlapping localization signals, namely an

72   N-myristoylation motif that tethers it to the plasma membrane (PM) and a chloroplast transit

73   peptide (cTP) that targets it to the chloroplast (Rosas-Diaz et al., 2018). While at least one of the

74   roles of C4 at the PM is to suppress the cell-to-cell movement of RNA interference (RNAi) (Rosas-

75   Diaz et al., 2018; Fan et al., 2019), the function of C4 in the chloroplast is so far enigmatic.

76   Here, we show that C4 shifts its localization from the PM to chloroplasts upon activation of immune

77   signalling by the replication-associated viral protein (Rep) or by exogenous treatments with the

78   bacterial peptide elicitor flg22 or the endogenous peptide Pep1. Once inside the organelle, C4

79   associates with the thylakoid transmembrane protein CAS. The effect of C4 is consistent with a

80   suppression of CAS function in retrograde signalling, as expression of this viral protein leads to

81   decreased CAS-dependent immune responses, namely lower amplitude in cytosolic calcium burst

82   upon pathogen perception, depressed transcriptional changes, reduced SA accumulation, and

83   compromised resistance against the plant pathogenic bacterium *Pseudomonas syringae*. The C4-

84   facilitated manipulation of chloroplast-mediated defences is biologically relevant, since knocking

85   down *CAS* or depleting downstream SA promotes viral accumulation and partially complements

86   a C4 null mutation in the virus, pointing at the suppression of SA responses as one of the main

87   roles of this virus-encoded protein.

88   Strikingly, we have found the coexistence of the overlapping targeting signals contained in C4,

89   the N-myristoylation site and the cTP, in a number of evolutionarily unrelated plant pathogen-

90   encoded effector proteins, including those from DNA viruses, RNA viruses, and bacteria.

91   Importantly, some of these effectors show dual membrane/chloroplast localization and suppress

92   chloroplast-dependent defences when targeted to this organelle. Moreover, co-occurrence of

93   these two targeting signals can also be found in a conserved set of plant proteins, many of which

94   have a described role in the regulation of defence responses. We demonstrate that one of these

95   proteins, Calcium Protein Kinase 16 (CPK16), re-localizes from the PM to chloroplasts upon flg22

96   treatment to promote chloroplast-dependent defences. Based on the results presented here, we

97   propose that a protein relocalization-dependent pathway physically linking PM and chloroplasts

98   and regulating defence exists in plants, and that this pathway has been co-opted by pathogens

99   during evolution to suppress defence responses and promote virulence.

100

101

RESULTS

The C4 protein from the geminivirus *Tomato yellow leaf curl virus* shifts its localization from the plasma membrane to chloroplasts upon activation of defence

When expressed in plant cells, the C4 protein from TYLCV fused to GFP at its C-terminus localizes preferentially at the PM, with a minor fraction visible in chloroplasts (Figure 1A, B; Rosas-Diaz et al., 2018). However, when co-expressed with a TYLCV infectious clone, C4-GFP strongly accumulates in chloroplasts and is depleted from the PM (Figure 1C); co-expression with the viral Replication-associated protein (Rep) alone, but not other virus-encoded proteins, is sufficient to trigger this shift in localization (Figure 1D). Expression of Rep in *Nicotiana benthamiana* leads to the activation of defence responses, probably owing to the recognition of the protein or its activity by the plant (Ding et al., 2019); in order to test whether activation of defence could lead to the re-localization of C4 from the PM to chloroplasts, we treated *N. benthamiana* leaves transiently expressing C4-GFP with the bacterial peptide elicitor flg22, which is recognized by a receptor complex at the cell surface and activates pattern-triggered immunity (PTI) (Felix et al., 1999; Gomez-Gomez and Boller, 2000). As shown in Figure 1E and Supplemental figure 1A, flg22 treatment results in a clear accumulation of C4-GFP in chloroplasts, at the expense of the PM pool; treatment with the translation inhibitor cycloheximide (CHX) supports the idea that the shift in PM/chloroplast C4-GFP accumulation ratio is due to physical re-localization of the protein, and not to differential targeting following synthesis *de novo*. The endogenous immunogenic peptide Pep1 similarly triggers the chloroplast re-localization of C4 in *N. benthamiana*, while treatment with the bacterial derived peptide elf18, for which *N. benthamiana* lacks a receptor, has no noticeable effect of the subcellular distribution of the protein (Supplemental figure 1B-D). The increase in chloroplast-localized C4-GFP following flg22 treatment can also be detected by organelle purification and western blot (Supplemental figure 1E); additionally, a 33 KDa variant of C4, corresponding to C4-GFP after the chloroplast import-coupled cleavage of the cTP (mature chloroplast form), accumulates at the expense of the full-length version of the fusion protein (Supplemental figure 1F). Chloroplast fractionation indicates that C4 is a peripheral thylakoid membrane protein facing the stroma (Figure 1F, G; Supplemental figure 1G). Nevertheless, accumulation of C4 in the chloroplast in transgenic Arabidopsis lines expressing the non-myristoylable C4$_{G2A}$ mutant version, which localizes to chloroplasts exclusively (Figure 1B; Rosas-Diaz et al., 2018), does not affect photosynthetic efficiency, chloroplast ultrastructure, or general plant development (Figure 1H-L).
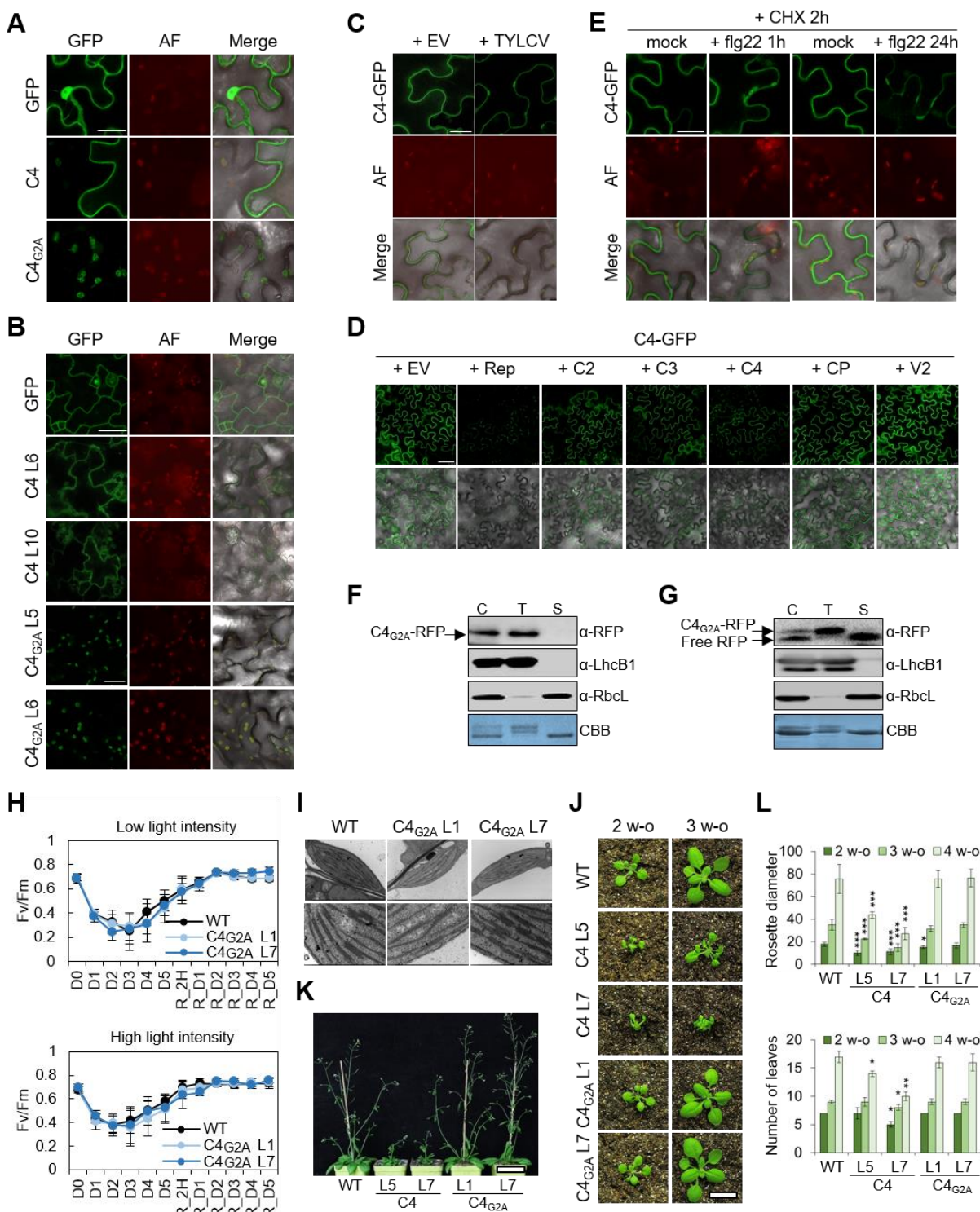
Figure 1. The C4 protein from the geminivirus TYLCV shifts its localization from plasma membrane to chloroplasts upon activation of defence. (**A**) C4 shows a plasma membrane (PM)/chloroplast dual localization upon transient expression in *N. benthamiana* leaves. Localization of the wild-type and the non-myristoylable (C4$_{G2A}$) C4 versions fused to GFP at two days post-infiltration (dpi). Scale bar = 25 μm. AF: Autofluorescence. (**B**) C4 shows a PM/chloroplast dual localization in Arabidopsis transgenic lines. Localization of the wild-type and the non-myristoylable

141　(C4$_{G2A}$) C4 versions fused to GFP in cotyledons of 7-day-old seedlings. Scale bar = 25 µm. AF: Autofluorescence. (**C**)
142　C4 re-localizes from PM to chloroplasts during TYLCV infection in *N. benthamiana* leaves. Localization of C4-GFP was
143　compared when expressed alone or co-infiltrated with a TYLCV infectious clone at 2dpi. Scale bar = 25 µm. AF:
144　Autofluorescence. (**D**) The virus-encoded Rep protein, but not other viral proteins, triggers chloroplast localization of
145　C4-GFP. C4-GFP was co-infiltrated with *Agrobacterium* clones to express each TYLCV protein independently in *N.*
146　*benthamiana* leaves and localization was determined at 2dpi. SMD settings: gating 1%, laser 10, gain 90%. With V2:
147　gating 1%, laser 10, gain 30%. EV: empty vector. Scale bar = 50 µm. (**E**) C4 re-localizes from PM to chloroplasts in
148　response to treatment with the bacterial peptide elicitor flg22 upon transient expression in *N. benthamiana* leaves.
149　Localization of C4-GFP was compared upon treatment with 1 µM flg22 or mock treatment (1h and 24 h post-treatment)
150　in the presence of CHX (50 µg/ml, 2 h). Scale bar = 25 µm. AF: Autofluorescence. (**F**) Transiently expressed C4$_{G2A}$-
151　RFP in *N. benthamiana* is associated to the chloroplast thylakoid membrane. Isolated chloroplasts were separated into
152　membrane and stroma fractions upon transient expression of the non-myristoylable C4 version (C4$_{G2A}$) fused to RFP
153　in *N. benthamiana* leaves (2dpi). (C: total chloroplast; T: thylakoid; S: stroma; LhcB1: light harvesting complex protein
154　B1 (25 kDa), a thylakoid membrane protein; RbcL: rubisco large subunit (52.7 kDa), a stromal protein). CBB: Comassie
155　brilliant blue. (**G**) Stably expressed C4$_{G2A}$-RFP in Arabidopsis is associated to the chloroplast thylakoid membrane.
156　Isolated chloroplasts from three-week-old Arabidopsis transgenic lines expressing the non-myristoylable C4 version
157　(C4$_{G2A}$) fused to RFP were separated into membrane and stroma fractions. (C: total chloroplast; T: thylakoid; S: stroma;
158　LhcB1: light harvesting complex protein B1 (25 kDa), a thylakoid membrane protein; RbcL: rubisco large subunit (52.7
159　kDa), a stromal protein). CBB: Comassie brilliant blue. (**H**) Chloroplast-localized C4 does not affect photosynthetic
160　efficiency. Ten-day-old wild-type or 35S:C4$_{G2A}$ (Lines 1 (L1) and 7 (L7)) seedlings were grown in ½ MS-sucrose agar
161　medium under constant light (low light intensity: 40 µmol m^{-2} s^{-1}; high light intensity: 80 µmol m^{-2} s^{-1}) for 5 days at 22°C,
162　followed by 5 days under constant light (very high intensity: 300 µmol m^{-2} s^{-1}) in cold stress conditions (10°C), when
163　Fv/Fm was recorded every day (D: day; D0 to D5: from day 0 to day 5); seedlings were then transferred to the initial
164　conditions (recovery), and Fv/Fm was recorded at the indicated time points (R: recovery; R_2h: 2 h after recovery;
165　R_D1 to R_D5: from day 1 to day 5 after recovery). (**I**) Chloroplast-localized C4 does not affect chloroplast ultrastructure.
166　Ten-day-old wild-type or 35S:C4$_{G2A}$ (Lines 1 (L1) and 7 (L7)) seedlings were grown in ½ MS -sucrose agar medium
167　under long day conditions and used for transmission electron microscopy imaging. (**J**) Expression of chloroplast-
168　localized C4 does not visibly affect development of 2- and 3-week-old transgenic Arabidopsis lines (Bar = 1 cm). (**K**)
169　Expression of chloroplast-localized C4 does not visibly affect development of five week-old transgenic Arabidopsis lines
170　(Bar = 7 cm). (**L**) Developmental phenotypes of transgenic Arabidopsis plants expressing C4 or C4$_{G2A}$ grown in long
171　day conditions. Rosette diameter is in mm. Bars represent SE of n = 3. Asterisks indicate a statistically significant
172　difference (*P < 0.05, **P < 0.01, ***P < 0.001) according to a one-way ANOVA with post-hoc Dunnett's multiple
173　comparisons test.

174

C4 interacts with Calcium Sensing Receptor in chloroplasts and suppresses downstream immune responses

177　Following activation of PTI, retrograde signalling allows communication of chloroplasts with the

178　nucleus, activating expression of genes required for the biosynthesis of the defense hormone

179　salicylic acid (SA) and ultimately leading to the accumulation of this compound (Qi et al., 2018;

180　Zhang and Li, 2019; Nomura et al., 2012). Since activation of PTI leads to the re-localization of

181　C4 from the PM to the chloroplast, and with the aim to detect a potential interference of C4 with

182　this signalling cascade, we measured the expression of SA biosynthetic and responsive genes

183　(*ICS1* and *PR1*, respectively) as well as the accumulation of SA after treatment with flg22 in

184　transgenic Arabidopsis plants expressing the chloroplast-localized C4$_{G2A}$ (Figure 2A,B and

185　Supplemental figure 2A). As shown in Figure 2A and B, the presence of C4 in the chloroplast

7

186 results in lower expression of SA-related genes and halved SA content after flg22 treatment. C4,
187 however, does not impair SA perception or downstream responses, as demonstrated by
188 exogenous SA treatments (Supplemental figure 2B). Importantly, the suppression of SA
189 biosynthesis seems to be relevant for the viral infection, in agreement with previous observations
190 (Li et al., 2019), since transgenic Arabidopsis or tomato plants depleted in SA (*NahG* transgenic
191 plants) support higher viral accumulation and can partially complement a null mutation in C4,
192 suggesting that the suppression of SA responses is one of the main functions of C4 in the context
193 of the infection (Figure 2C, Supplemental figure 2C).

194 We reasoned that the C4-mediated hampering of immune chloroplast retrograde signalling could
195 be most likely based on the interaction with some plant protein, hence we performed affinity
196 purification followed by mass spectrometry analysis (AP-MS) upon transient expression of $C4_{G2A}$
197 in *N. benthamiana* to identify potential interactors of the chloroplast-localized C4. This approach
198 unveiled the plant-specific Calcium Sensing Receptor (CAS) as a putative interactor of C4 in the
199 chloroplast (Figure 2D); this protein-protein interaction was subsequently confirmed by
200 bimolecular fluorescent complementation (BiFC) and co-immunoprecipitation (co-IP) analyses
201 (Figure 2E, F). CAS is described as a thylakoid membrane-spanning protein (Nomura et al., 2012;
202 Cutolo et al., 2019); topology analyses demonstrate that the C-terminus of CAS faces the stroma
203 and interacts with C4, itself associated to the thylakoid membrane as peripheral protein (Figure
204 2F,G and Supplemental figure 2D-F). Interestingly, CAS has been previously demonstrated to be
205 required for retrograde signalling in PTI and the ensuing activation of SA biosynthesis (Nomura
206 et al., 2012). Therefore, we next tested known CAS-dependent responses to flg22 in our
207 transgenic lines expressing chloroplast-localized C4. As shown in Figure 2H-K, plants expressing
208 $C4_{G2A}$ display immune defects at different levels, including reduced cytoplasmic calcium burst
209 (Figure 2H and Supplemental figure 2G), lower callose deposition (Figure 2I), defective
210 transcriptional reprogramming (Figure 2J and Supplemental figure 2H), and increased
211 susceptibility to *P. syringae* pv. *tomato* DC3000 (Figure 2K and Supplemental figure 2I), all of
212 them phenocopying a *cas* mutant and hence consistent with an inhibition of this protein. Of note,
213 and as expected, flg22 perception is not affected in $C4_{G2A}$ transgenic lines or in a *cas* mutant,
214 since the early apoplastic burst of reactive oxygen species (ROS) as well as the late seedling
215 growth inhibition occur normally in these plants in response to the peptide treatment
216 (Supplemental figure 2J, K; Nomura et al., 2012). The biological relevance of the potential C4-
217 mediated inhibition of CAS is illustrated by the fact that a *cas* Arabidopsis mutant as well as *N.*
218 *benthamiana* or tomato plants in which *CAS* has been knocked down by virus-induced gene

8

219   silencing (VIGS) are all more susceptible to TYLCV infection, indicating that suppression of CAS

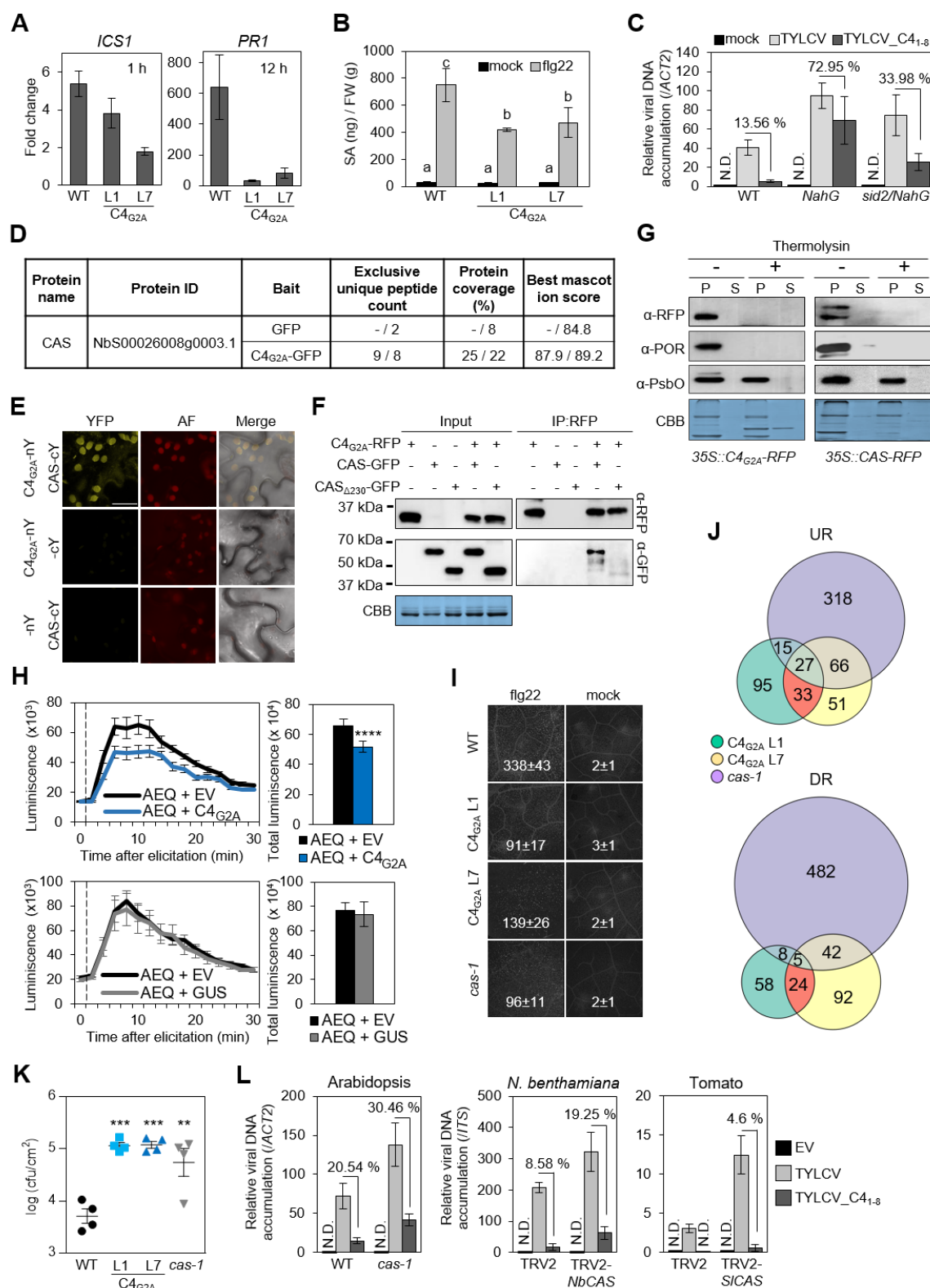220   function has a positive impact on the virus' performance (Figure 2L and Supplemental figure 2L).

221

222 **Figure 2. Chloroplast-localized C4 interacts with Calcium sensing receptor (CAS) and suppresses downstream**
223 **immune responses.** (**A**) Chloroplast-localized C4 suppresses retrograde signalling. Flg22-induced *ICS1* and *PR1*
224 expression was analysed in ten-day-old wild-type or transgenic Arabidopsis lines expressing C4$_{G2A}$ at the indicated
225 time points by qRT–PCR. Seedlings were grown on ½ MS agar plates under long day conditions prior to transfer to
226 liquid ½ MS for elicitation. *ACT2* was used as the normalizer. Data are mean ± SE of three independent biological
227 replicates. (**B**) Chloroplast-localized C4 suppresses SA accumulation upon flg22 treatment. Total SA content was
228 quantified in ten-day-old wild-type or transgenic Arabidopsis lines expressing C4$_{G2A}$. Seedlings were grown on ½ MS
229 agar plates under long day conditions prior to transfer to liquid ½ MS for elicitation with 1 µM flg22 during 12 h. Data
230 are mean ± SE of three independent biological replicates. Lowercase letters indicate statistically significant differences
231 between mean values (P <0.001), according to a one-way ANOVA with post-hoc Tukey's multiple comparisons test.
232 (**C**) Viral accumulation in Arabidopsis *NahG* and *sid2/NahG* plants infected with TYLCV wild type (TYCLV) or a mutant
233 version carrying a premature stop codon in position 9 of the C4 gene (TYLCV_C4$_{1-8}$). The relative viral DNA
234 accumulation in plants was determined by qPCR of total DNA extracted from the six youngest rosette leaves at 21 days
235 post-inoculation (dpi). Values represent the average of eight plants. Error bars represent SE. ND: not detectable. "%"
236 indicates the percentage of TYLCV_C4$_{1-8}$ accumulation compared to TYLCV (100%). Experiments were repeated at
237 least three times with similar results; data from one biological replicate are shown. (**D**) CAS peptides identified in affinity
238 purification-mass spectrometry (AP-MS) analysis after purification of C4$_{G2A}$-GFP and GFP from *N. benthamiana* leaves
239 in two independent experiments. "-" indicates no peptide was detected. (**E**) Biomolecular fluorescence complementation
240 (BiFC) assay showing the interaction between C4$_{G2A}$ and CAS. YFP fluorescence was observed in chloroplasts upon
241 transient co-expression in *N. benthamiana* leaves at 2 dpi. Scale bar = 25 µm. AF: Autofluorescence. (**F**) C4$_{G2A}$ interacts
242 with the C-terminal part of CAS by co-immunoprecipitation upon transient co-expression in *N. benthamiana* leaves.
243 Full-length or a truncated version of CAS lacking the rhodanese-like domain (CAS$_{\Delta230}$) were used. Molecular weight is
244 indicated. CBB: Comassie brilliant blue. (**G**) Topology analysis of chloroplast-localized C4 and CAS proteins.
245 Thermolysin digestion of freshly isolated thylakoid membranes indicates that chloroplastic C4 is a stroma-facing
246 thylakoid peripheral protein that interacts with the stroma-facing C-terminal part of CAS (P: thylakoid pellet; S:
247 supernatant; POR: protochlorophyllide oxidoreductase (37 kDa), a thylakoid peripheral protein towards stroma; PsbO:
248 photosystem II subunit O (33 kDa), a lumen localized protein). CBB: Comassie brilliant blue. (**H**) Chloroplast-localized
249 C4 impairs the CAS-dependent cytoplasmic calcium transient in response to flg22. The calcium sensor aequorin (AEQ)
250 was transiently co-expressed with C4$_{G2A}$ or GUS (as negative control) in *N. benthamiana* leaves. The vertical dashed
251 lines indicate the time at which treatment was initiated. AEQ luminescence was recorded during 30 min every two
252 minutes (luminiscence in cp 120^{-s}). Total luminescence was calculated at the end of the experiment. Values represent
253 the average of six plants. Error bars represent SE. Asterisks indicate a statistically significant difference (****P < 0.0001)
254 according to a two-tailed comparisons t-test. This experiment were repeated at least three times with similar results;
255 data from one experiment are shown. EV: empty vector. (**I**) Chloroplast-localized C4 impairs flg22-induced callose
256 deposition. Representative pictures and the average number (with SD) of callose deposits per 2.5 mm^2 (n=10) are
257 shown. This experiment was repeated three times with similar results; results from one experiment are shown. (**J**)
258 Transcriptional overlap between transgenic Arabidopsis plants expressing C4$_{G2A}$ and a *cas-1* mutant upon activation
259 of plant immunity by treatment with the bacterial peptide elicitor flg22 (1 µM, 12 h). RNA-seq data were obtained from
260 ten-day-old Arabidopsis seedlings grown on ½ MS agar plates under long-day conditions prior to transfer to ½ MS
261 liquid for elicitation. UR: up-regulated; DR: down-regulated. Comparisons are made with treated control (wild-type)
262 plants. (**K**) Transgenic Arabidopsis plants expressing C4$_{G2A}$ display increased susceptibility to the bacterial pathogen
263 *P. syringae* pv. *tomato* DC3000. Four-week-old short-day-grown plants were inoculated by infiltration with *Pto*DC3000.
264 Three days later, bacteria were extracted from 7-mm leaf discs from three different leaves of four independent plants
265 and incubated at 28 °C for two days. Data are mean ± SE of n = 4. This experiment was repeated 3 times with similar
266 results; results from one experiment are shown. Asterisks indicate a statistically significant difference (**P < 0.01, ***P
267 < 0.001) according to a one-way ANOVA with post-hoc Dunnett's multiple comparisons test. (**L**) Mutation in *CAS*
268 favours infection by TYLCV and partially complements a C4 null mutant virus. Relative accumulation of TYLCV wild
269 type (TYCLV) or a mutant version carrying a premature stop codon in position 9 of the C4 gene (TYLCV_C4$_{1-8}$) in *cas-*
270 *1* Arabidopsis plants and *N. benthamiana* and tomato plants in which *CAS* has been silenced by VIGS, as determined
271 by qPCR. Total DNA was extracted from the 6 youngest apical leaves in Arabidopsis and from the 2 youngest apical
272 leaves in *N. benthamiana* and tomato, at 21 dpi. Values represent the average of 6 plants. Error bars represent SE.
273 ND: not detectable. EV: empty vector. Experiments were repeated at least three times with similar results; results from
274 one experiment are shown.

10

Proteins encoded by evolutionarily unrelated pathogens contain overlapping membrane- and chloroplast-targeting signals and suppress chloroplast-mediated defences

Our results show that the geminivirus TYLCV has evolved a strategy, through the action of the virus-encoded C4 protein and its shuttling from the PM to the chloroplast, to interfere with chloroplast-mediated SA-dependent defence responses and promote viral performance. Since SA has been proven to counter virus infection in different plant-virus interactions (e.g. Chen et al., 2010; Ji et al., 2001; Kachroo et al., 2000; Malamy et al., 1990) and chloroplasts are crucial players in this pathway, we hypothesized that other plant viruses might have independently evolved similar strategies to target this organelle when they are perceived by the plant. In an attempt to identify such hypothetical proteins, we searched public databases for proteins encoded by plant viruses containing both an N-myristoylation motif and a cTP. Surprisingly, we found ~400 viral proteins in which these two localization signals co-exist, encoded by viral species belonging to four different families (Figure 3A); most of these proteins are encoded by geminiviruses (Supplemental figure 3A). From this set of proteins, we selected four to test the functionality of their localization signals as well as their biological effect following chloroplast localization: C4 from the curtovirus *Beet curly top virus* (BCTV) (Fam. *Geminiviridae*); AC4 from the bipartite begomovirus *East African cassava mosaic virus* (EACMV) (Fam. *Geminiviridae*); the capsid protein (CP) from the cucumovirus *Cucumber mosaic virus* (CMV) (Fam. *Bromoviridae*); and the P3 protein from the nepovirus *Grapevine fanleaf virus* (GFLV) (Fam. *Secoviridae*) (Supplemental figure 3B). In all cases, the wild-type version of these viral proteins fused to GFP transiently expressed in *N. benthamiana* appeared as associated to membranes, while the non-myristoylable (G2A) mutant versions accumulated in the chloroplast (Figure 3B). Treatment with flg22 triggered the re-localization of C4 from BCTV and AC4 from EACMV to chloroplasts; this effect could not be clearly observed for CP and P3, suggesting that a different signal might be required in these two cases (Figure 3C). We next tested immune readouts in *N. benthamiana* leaves transiently expressing the chloroplast-localized (G2A) version of these proteins. Strikingly, the chloroplastic versions of all four viral proteins reduced the expression of *NbICS1*, *NbPR1*, and other defence-related genes, as well as the cytosolic calcium burst, in response to flg22, while all but P3 enhanced susceptibility against the pathogenic bacteria *P. syringae* pv tomato DC3000 *ΔhopQ1* (Figure D-F, Supplemental figure 3C-E), indicating that these phylogenetically unrelated viral effectors are capable of interfering with SA-mediated defences from the chloroplast. Expression of these proteins does not interfere with the apoplastic ROS burst that follows flg22 treatment, indicating that perception of the PAMP occurs normally (Figure 3G, Supplemental figure 3F).
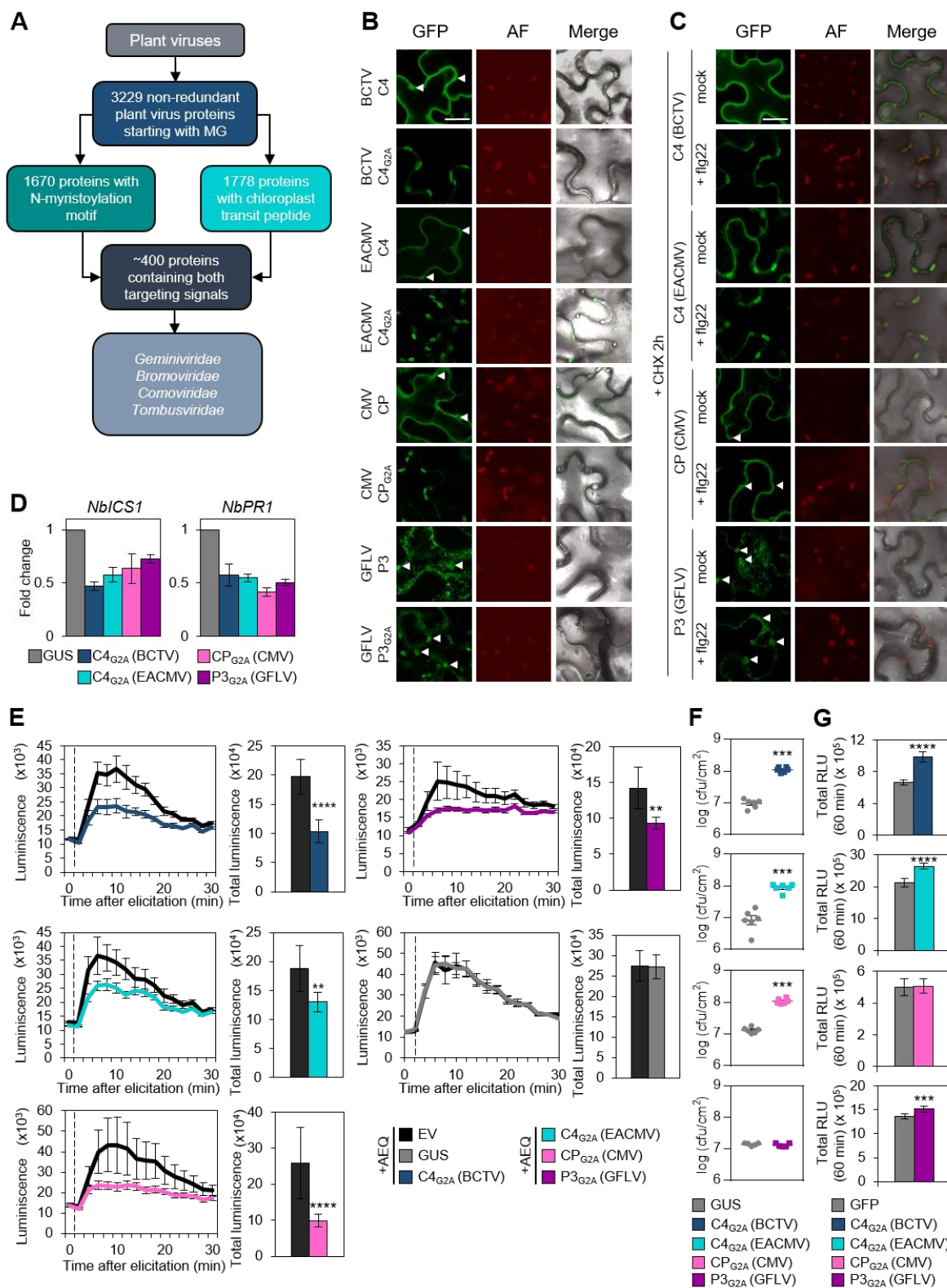
11

308

Figure 3. Proteins encoded by plant viruses contain overlapping membrane- and chloroplast-targeting signals and suppress chloroplast-mediated defences. (**A**) Flow diagram illustrating the number of proteins encoded by plant viruses and containing an N-myristoylation motif, a chloroplast transit peptide, or both, and the families they belong to.

312 (**B**) Selected viral proteins with overlapping N-myristoylation motif and cTP (C4 from the curtovirus *Beet curly top virus*
313 (BCTV; Fam. *Geminiviridae*); AC4 from the bipartite begomovirus *East African Cassava Mosaic Virus* (EACMV; Fam.
314 *Geminiviridae*); the capsid protein (CP) from the cucumovirus *Cucumber mosaic virus* (CMV; Fam. *Bromoviridae*); and
315 the P3 protein from the nepovirus *Grapevine fanleaf virus* (GFLV; Fam. *Secoviridae*) show PM/chloroplast dual
316 localization upon transient expression in *N. benthamiana* leaves. Localization of the wild-type proteins and the non-
317 myristoylable (G2A) versions fused to GFP was observed at two days post-infiltration (dpi). Scale bar = 25 μm. AF:
318 Autofluorescence. This experiment was repeated 3 times with similar results. Arrowheads indicate chloroplasts. (**C**)
319 Geminiviral proteins with overlapping N-myristoylation motif and cTP (C4 from BCTV and AC4 from EACMV) re-localize
320 to chloroplasts upon activation of immunity. Localization of the wild-type proteins was monitored under different
321 conditions (mock vs. 1 μM flg22, 24 h post-treatment). Scale bar = 25 μm. AF: Autofluorescence. This experiment was
322 repeated 3 times with similar results. Arrowheads indicate chloroplasts. (**D**) Viral proteins with the overlapping N-
323 myristoylation motif and cTP suppress expression of SA-related genes upon activation of plant immunity in *N.*
324 *benthamiana* leaves. PAMP treatment (1 μM flg22) was performed 48 h after transient transformation. Leaf discs from
325 three plants were collected separately 9 hours after treatment. Gene expression was analysed by qRT–PCR. *NbEF1α*
326 was used as an internal standard. Values represent the average of 4 independent experiments with 3 plants used in
327 each replicate. Data are mean ± SE of three independent experiments. (**E**) Chloroplast-localized viral proteins impair
328 the CAS-dependent cytoplasmic calcium transient in response to flg22. The calcium sensor aequorin (AEQ) was
329 coexpressed with the untagged non-myristoylable (G2A) versions of the viral proteins or GUS (as a negative control)
330 in *N. benthamiana* leaves. The vertical dashed lines indicate the time at which flg22 treatment was initiated. AEQ
331 luminescence was recorded during 30 min every two minutes (luminiscence in cp 120^{-s}). Total luminescence was
332 calculated at the end of the experiment. Values represent the average of 6 plants. Error bars represent SE. Asterisks
333 indicate a statistically significant difference (**P < 0.01, ****P < 0.0001) according to a two-tailed comparisons t-test.
334 Experiments were repeated at least three times with similar results; results from one experiment are shown. EV: empty
335 vector. (**F**) Chloroplast-localized viral proteins increase susceptibility to the plant pathogenic bacterial strain *P. syringae*
336 pv. *tomato* DC3000 Δ*hopQ1-1*. Leaves of four-week-old *N. benthamiana* plants were inoculated by infiltration with a
337 *Pto*DC3000Δ*hopQ1-1* suspension 24 h after transient transformation. Three days later, bacteria were extracted from
338 7-mm leaf discs from two different leaves of 3 independent plants and incubated at 28 °C for 2 days. Data are mean ±
339 SE. Asterisks indicate a statistically significant difference (***P < 0.001) according to a two-tailed comparisons t-test.
340 Experiments were repeated at least three times with similar results; results from one experiment are shown. (**G**) Total
341 ROS production in the 60 min following flg22 treatment in *N. benthamiana* leaves 48 h after transient transformation.
342 Error bars indicate SE (n = 24). Asterisks indicate a statistically significant difference (***P < 0.001, ****P < 0.0001)
343 according to a two-tailed comparisons t-test. Experiments were repeated at least three times with similar results; results
344 from one experiment are shown.

345

346 Given that viral proteins from independent origins show a similar coexistence of targeting signals

347 and share the capacity to interfere with SA-dependent defences from the chloroplast, and

348 considering the general effect of SA on different plant-pathogen interactions, we next sought to

349 answer the question of whether unrelated plant pathogens such as bacteria can encode effector

350 proteins with a similar localization pattern and effect. With this purpose, we screened the entire

351 predicted proteome of the plant pathogenic bacterium *Ralstonia solanacearum* GMI1000 for

352 proteins containing both an N-myristoylation motif and a cTP. This search yielded 2 proteins

353 (GALA1 and GALA3) (Figure 4A, Supplementary figure 4A). Interestingly, both proteins have

354 been described as effector proteins secreted inside plant cells during bacterial infection

355 (Mukaihara et al, 2010).

13

356   For subsequent functional characterization, we selected *R. solanacearum* GALA1, since GALA3

357   could not be detected by confocal microscopy upon transient expression in *N. benthamiana*

358   leaves. GALA1-GFP presented the predicted dual PM/chloroplast localization, and its

359   accumulation in the chloroplast increased upon treatment with flg22 (Figure 4B, C and

360   Supplemental figure 4B). Nevertheless, both bacterial effectors, GALA1 and GALA3, could be

361   detected in chloroplasts upon expression of their G2A version fused to GFP following organelle

362   purification and IP (Supplemental figure 4C). Importantly, chloroplast accumulation of either of

363   these effectors led to a reduction in the cytoplasmic calcium burst in response to flg22 treatment

364   (Figure 4D and Supplemental figure 4D). Since *R. solanacearum* is capable of efficiently infecting

365   Arabidopsis, we generated stable transgenic Arabidopsis plants expressing GALA1$_{G2A}$ or

366   GALA3$_{G2A}$ fused to GFP, which showed the expected chloroplast localization (Supplemental

367   figure 4E, F). These plants display altered expression of SA-responsive genes following flg22

368   treatment, and are more susceptible to *P. syringae* pv. *tomato* DC3000 (Figure 4E-G and

369   Supplemental figure 4G), indicating that these bacterial effector proteins can disturb SA-

370   dependent defences when localized in the chloroplast. Nevertheless, perception of flg22 is not

371   affected by the expression of the chloroplast-localized versions of these bacterial effectors, since

372   production of apoplastic ROS upon elicitation with the peptide occurs normally (Figure 4H,
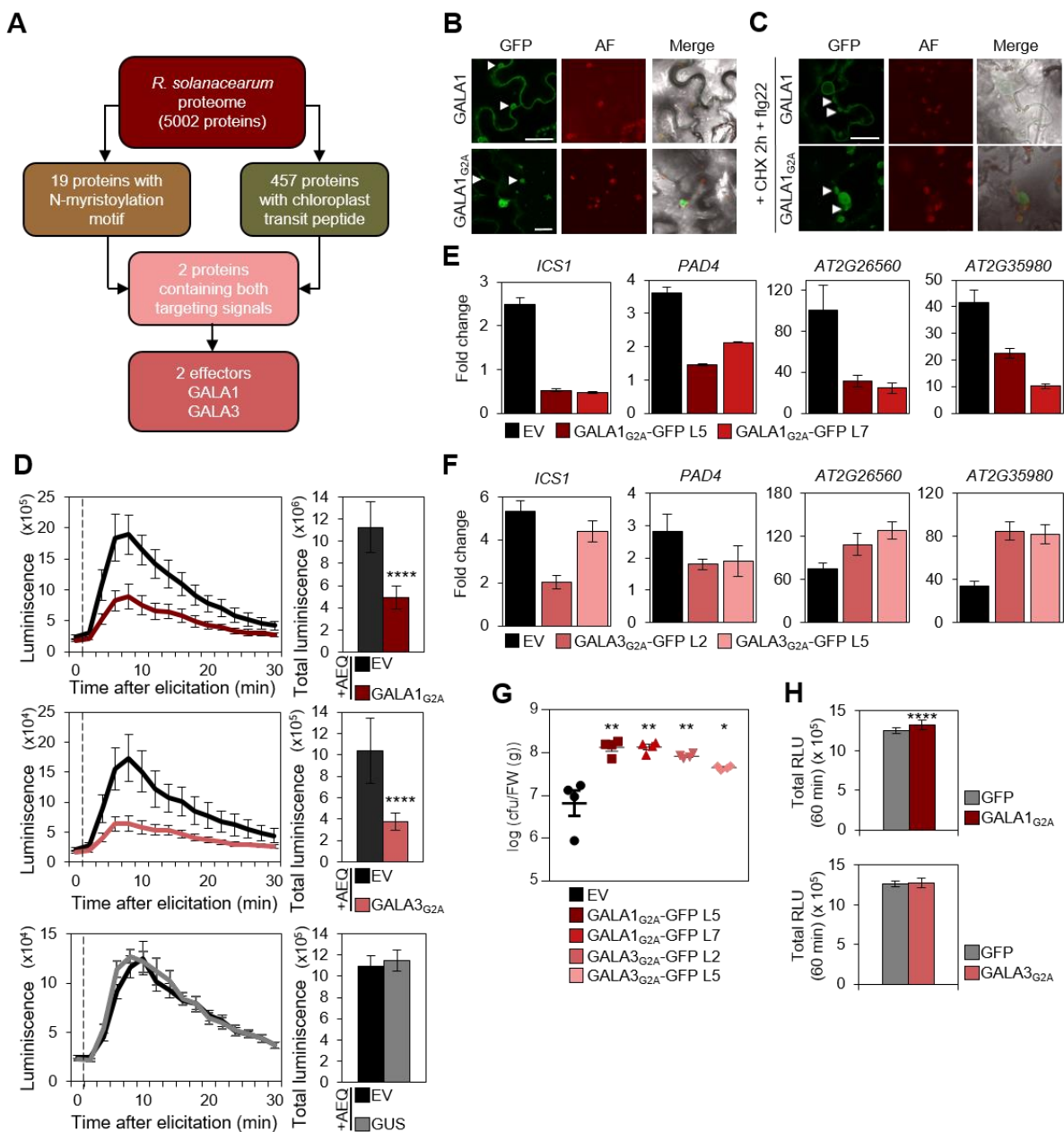
373   Supplemental figure 4H).

374

Figure 4. Effector proteins from plant pathogenic bacteria contain overlapping membrane- and chloroplast-targeting signals and suppress chloroplast-mediated defences. (**A**) Flow diagram illustrating the number of proteins encoded by the plant pathogenic bacterial strain *Ralstonia solanacearum* (GMI1000) and containing an N-myristoylation motif, a chloroplast transit peptide, or both. (**B**) The effector GALA1 from *R. solanacearum* GMI1000, which contains overlapping N-myristoylation motif and cTP, shows PM/chloroplast dual localization in *N. benthamiana* leaves. Localization of the wild-type (GALA1) and the non-myristoylable (GALA1$_{G2A}$) versions fused to GFP was observed 2 days post-infiltration. Scale bar = 25 µm. AF: Autofluorescence. Arrowheads indicate chloroplasts. (**C**) GALA1 re-localizes to chloroplasts upon activation of immunity. Localization of the wild-type (GALA1) version fused to GFP was monitored 24 h upon activation of plant immunity by treating with 1 µM flg22. Scale bar = 25 µm. AF: Autofluorescence. Arrowheads indicate chloroplasts. (**D**) Chloroplast accumulation of GALA1 and GALA3 impairs the CAS-dependent cytoplasmic calcium transient in response to flg22. The calcium sensor aequorin (AEQ) was co-expressed with the non-myristoylable (G2A) versions of GALA1 and GALA3 or GUS (as negative control) in *N.*

388 *benthamiana* leaves. The vertical dashed lines indicate the time at which flg22 treatment was initiated. AEQ
389 luminescence was recorded during 30 min every two minutes (luminiscence in cp 120^{-s}). Total luminescence was
390 calculated at the end of the experiment. Values represent the average of 6 plants. Error bars represent SE. Asterisks
391 indicate a statistically significant difference (****$P < 0.0001$) according to a two-tailed comparisons t-test. Experiments
392 were repeated at least three times with similar results; results from one experiment are shown. EV: empty vector. (**E**)
393 Chloroplast-localized GALA1 hampers expression of SA biosynthetic and CAS-dependent genes upon activation of
394 plant immunity. Flg22-induced gene expression was analysed in 10-day-old Arabidopsis transgenic lines expressing
395 GALA1$_{G2A}$-GFP 1 h after flg22 treatment by qRT–PCR. Seedlings were grown under long-day conditions on ½ MS agar
396 plates prior to their transfer to liquid ½ MS for elicitation with 1 µM flg22. *ACT2* was used as the normalizer. Data are
397 mean ± SE of three independent biological replicates with three technical replicates each. EV: empty vector. (**F**)
398 Chloroplast-localized GALA3 hampers expression of SA biosynthetic genes but enhances the expression of CAS-
399 dependent genes upon activation of plant immunity. Flg22-induced gene expression was analysed in 10-day-old
400 Arabidopsis transgenic lines expressing GALA3$_{G2A}$-GFP 1 h after flg22 treatment by qRT–PCR. Seedlings were grown
401 under long day conditions on ½ MS agar plates prior to their transfer to liquid ½ MS for elicitation with 1 µM flg22. *ACT2*
402 was used as the normalizer. Data are mean ± SE of three independent biological replicates with three technical
403 replicates each. EV: empty vector. (**G**) Transgenic Arabidopsis plants expressing chloroplast-localized GALA1 or
404 GALA3 (GALA1$_{G2A}$ and GALA3$_{G2A}$ plants) display increased susceptibility to the bacterial pathogen *P. syringae* pv.
405 *tomato* DC3000. Three-week-old short-day-grown plants were spray-inoculated with *Pto*DC3000. Three days later,
406 bacteria were extracted from 4 independent plants and incubated at 28 °C for 2 days. Data are mean ± SE of n = 4.
407 This experiment was repeated 4 times with similar results; results from one experiment are shown. Asterisks indicate
408 a statistically significant difference (*$P < 0.05$, **$P < 0.01$) according to a one-way ANOVA with post-hoc Dunnett's
409 multiple comparisons test. EV: empty vector. (**H**) Total ROS production in the 60 min following flg22 treatment in *N.*
410 *benthamiana* leaves 48 h after transient transformation. Error bars indicate SE (n = 24). Asterisks indicate a statistically
411 significant difference (****$P < 0.0001$) according to a two-tailed comparisons t-test. Experiments were repeated at least
412 three times with similar results; results from one experiment are shown.

413

The plant-encoded CPK16 employs overlapping targeting signals to re-localize from PM to chloroplasts and promote chloroplast-mediated immune signalling

416 The finding that pathogens from different kingdoms of life seem to have convergently evolved to
417 target chloroplasts and impair SA-dependent defences following a previous association with
418 membranes raises the idea that a pathway linking PM to chloroplasts might exist in plants, and
419 that such pathway might have been co-opted by different plant pathogens during host-pathogen
420 co-evolution. Following this rationale, we decided to screen the predicted Arabidopsis proteome
421 to identify proteins containing both an N-myristoylation motif and a cTP, and found 78 proteins
422 fulfilling this criterion (Figure 5A; Supplemental table 1). Interestingly, functional enrichment
423 analysis of this subset of proteins unveiled an over-representation of defence regulators and
424 protein kinases (Supplemental figure 5A). We next performed a similar screen using the predicted
425 tomato and rice proteomes, and found 68 and 107 proteins containing both localization signals,
426 respectively (Supplemental figure 5B,C; Supplemental tables 2 and 3), among which defence
427 regulators and protein kinases are also over-represented (Supplemental figure 5D,E). Strikingly,
428 comparison of the identified proteins in Arabidopsis, tomato, and rice yielded a core of 26
429 homologous proteins common to all three species and containing an N-myristoylation site and a

16

430   cTP (Table 1; Figure 5B), which shows an over-representation of proteins described as involved

431   in SA signalling and systemic acquired resistance as well as protein kinases (Figure 5C). Of note,

432   the green algae *Chlamydomonas reinhardtii*, the liverwort *Marchantia polymorpha*, and the moss

433   *Physcomitrella patens* also encode proteins containing the N-myristoylation motif and the cTP (19,

434   30, and 21, respectively; Supplementary figure 5F; Supplementary tables 4, 5, and 6), with a

435   significant over-representation of protein kinases (Supplementary figure 5G-I).

436   Among the proteins identified in Arabidopsis, one of them, Calcium-Dependent Kinase 16

437   (CPK16), had already been shown to associate to the PM in an N-myristoylation motif-dependent

438   manner and to harbour a functional cTP (Stael et al., 2011); however, chloroplast localization

439   could be observed only upon mutation of the myristoylation site, and hence its biological

440   significance was unclear. Following transient expression in *N. benthamiana*, CPK16-GFP could

441   be observed mostly at the PM, while, as previously described, a $CPK16_{G2A}$ mutant version was

442   detected in chloroplasts (Figure 5D); stable expression in Arabidopsis yielded similar results

443   (Figure 5E). However, after flg22 treatment, CPK16-GFP accumulated in chloroplasts, similarly

444   to C4-GFP (Figure 5F, Supplemental figure 5J); chloroplast localization could still be detected

445   after CHX treatments, indicating that this process does not require new protein synthesis, and

446   therefore the chloroplast-localized protein most likely derive from the PM pool (Figure 5F).

447   As proof-of-concept, we decided to investigate whether CPK16 plays a role in PTI responses

448   when localized in the chloroplast. For this purpose, we generated transgenic Arabidopsis lines

449   expressing wild-type CPK16 or its chloroplast-localized $CPK16_{G2A}$ version under the 35S

450   promoter (Supplemental figure 5K); these transgenic lines had no obvious developmental

451   phenotype (Supplemental figure 5L). Following flg22 treatment, both CPK16 and $CPK16_{G2A}$ plants

452   displayed normal ROS burst but enhanced expression of SA marker genes (*ICS1*, *PAD4*, and

453   *PR1*), an effect that was more pronounced for early-expressing genes when the chloroplastic

454   version of CPK16 was used (Figure 5G, H; Supplemental figure 5M). Although a moderate

455   increase in the amplitude of the flg22-triggered cytoplasmic calcium burst could be detected in *N.*

456   *benthamiana* as the result of CPK16 overexpression, $CPK16_{G2A}$ had no evident effect on this

457   readout (Figure 5I, Supplemental figure 5N). Importantly, both CPK16- and $CPK16_{G2A}$-

458   overexpressing lines are also more resistant to *P. syringae* pv tomato DC3000 (Figure 5J,

459   Supplementary figure 5O), indicating that CPK16 contributes to anti-bacterial immunity from the
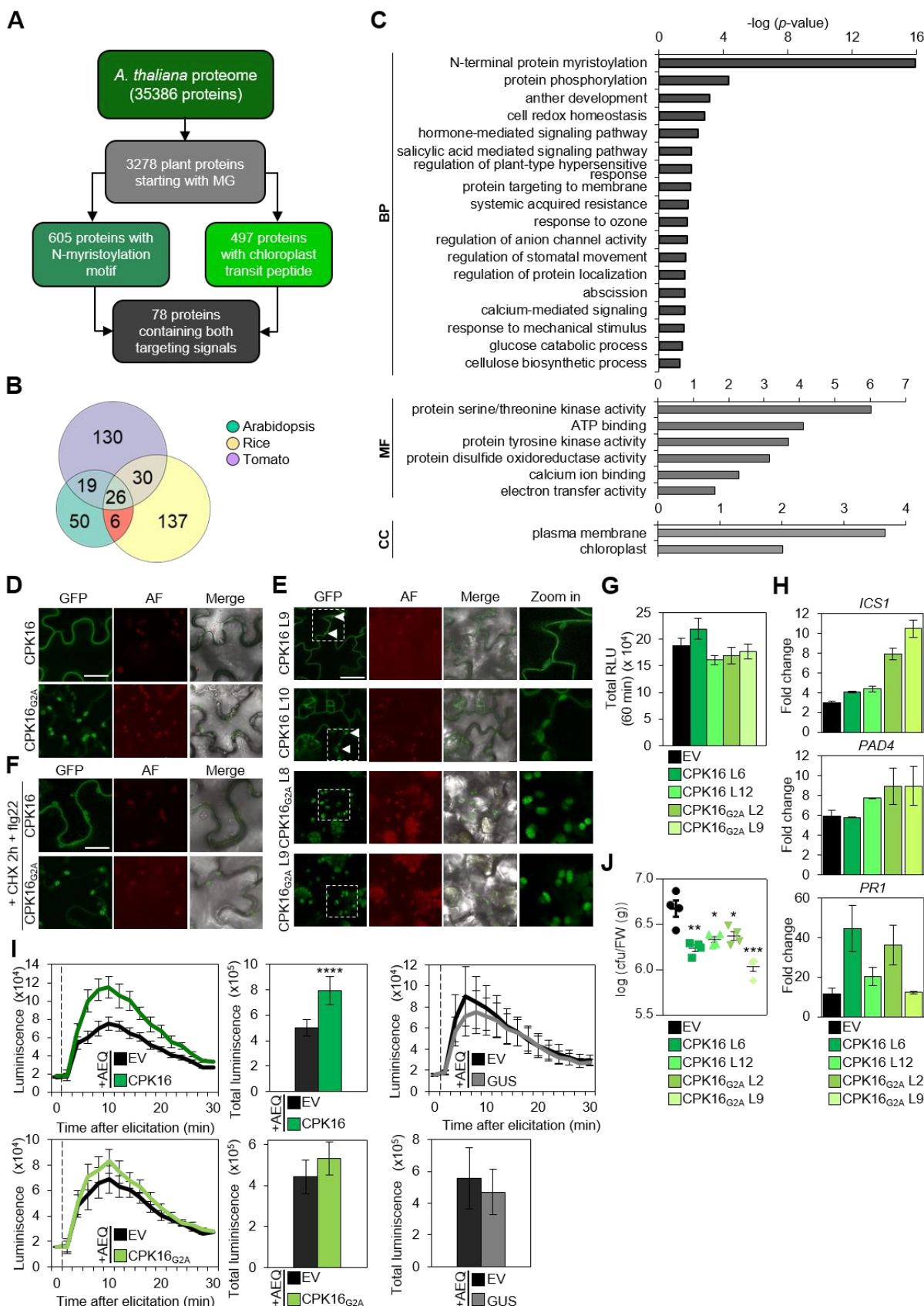
460   chloroplast.

Figure 5. The plant Calcium protein kinase 16 (CPK16) contains overlapping plasma membrane- and chloroplast-targeting signals, shifts its localization from plasma membrane to chloroplasts upon activation of defence, and activates chloroplast-mediated defences. (**A**) Flow diagram illustrating the number of proteins encoded by *Arabidopsis thaliana* containing an N-myristoylation motif, a chloroplast transit peptide, or both. (**B**) Venn diagram of proteins with overlapping N-myristylation motifs and cTPs in the predicted proteomes of Arabidopsis, tomato, and rice. (**C**) The subset of 26 common proteins containing overlapping N-myristylation motifs and cTPs in the predicted proteomes of Arabidopsis, tomato, and rice is enriched in defence-related GO terms. BP: biological process ontology; MF: molecular function ontology; CC: cellular component ontology. (**D**) CPK16 shows PM localization upon transient expression in *N. benthamiana* leaves. Localization of the wild-type (CPK16) and the non-myristoylable (CPK16$_{G2A}$) versions fused to GFP was observed at 2 days post-infiltration. Scale bar = 25 μm. AF: Autofluorescence. (**E**) CPK16 shows PM/chloroplast dual localization in transgenic 5-day-old *A. thaliana.* Localization of the wild-type (CPK16) and the non-myristoylable (CPK16$_{G2A}$) versions fused to GFP is shown. Scale bar = 25 μm. AF: Autofluorescence. Dashed squares indicate region of interest corresponding to the zoom-in panels. Arrowheads indicate chloroplasts. (**F**) CPK16 re-localizes from the PM to the chloroplasts upon activation of PTI in *N. benthamiana* leaves. CPK16 localization was monitored 12 h after activation of PTI by treatment with 1 μM flg22. Scale bar = 25 μm. AF: Autofluorescence. This experiment was repeated three times with similar results. (**G**) Total ROS production in the 60 min following flg22 treatment in *N. benthamiana* leaves 48 h after transient transformation. Error bars indicate SE (n = 16). (P = 0.666, according to a one-way ANOVA). Experiments were repeated at least three times with similar results; results from one experiment are shown. EV: empty vector. (**H**) Constitutive chloroplast localization of CPK16 in transgenic CPK16$_{G2A}$ *A. thaliana* plants promotes expression of defence-related marker genes upon activation of defence. Gene expression was analysed 1 h after 1 μM flg22 treatment by qRT–PCR. Seedlings were grown under long-day conditions on ½ MS agar plates prior to their transfer to liquid ½ MS for elicitation. *ACT2* was used as the normalizer. Data are mean ± SE of three independent biological replicates with three technical replicates each. EV: empty vector. (**I**) CPK16 modulates calcium-burst upon activation of plant immunity. The calcium sensor aequorin (AEQ) was coexpressed with the untagged versions of CPK16 or GUS (as negative control) in *N. benthamiana* leaves. The vertical dashed lines indicate the time at which treatment was initiated. AEQ luminescence was recorded during 30 min every two minutes (luminiscence in cp 120^{-s}). Total luminescence was calculated at the end of the experiment. Values represent the average of 6 plants. Error bars represent SE. Asterisks indicate a statistically significant difference (****P < 0.0001) according to a two-tailed comparisons t-test. Experiments were repeated at least three times. Representative data are shown. EV: empty vector. (**J**) Transgenic Arabidopsis plants overexpressing CPK16 or CPK16$_{G2A}$ display increased resistance against the bacterial pathogen *P. syringae* pv. *tomato* DC3000. Three-week-old short-day-grown plants were spray-inoculated with *Pto*DC3000. Three days later, bacteria were extracted from 4 independent plants and incubated at 28 °C for 2 days. Data are mean ± SE of n = 4. This experiment was repeated 4 times with similar results; results from one experiment are shown. Asterisks indicate a statistically significant difference (*P < 0.05, **P < 0.01, ***P < 0.001) according to a one-way ANOVA with post-hoc Dunnett's multiple comparisons test. EV: empty vector.

DISCUSSION

It has become widely recognized that, in addition to their function as energy providers, chloroplasts play an essential role in different aspects of plant biology as stress sensors and signal integrators; however, how these organelles, which reside inside the cell separated from the cytosol by a double membrane, can sense external cues is a long-standing question.

Taken together, the results presented here suggest the existence of a novel conserved pathway in plants that physically connects the PM and chloroplasts through protein re-localization upon a specific trigger, namely the perception of a biotic threat (Figure 6). This pathway, exemplified by CPK16, would involve proteins harbouring two overlapping and conflicting targeting signals: an

19

507 N-myristoylation site, tethering the protein to the PM, and a cTP, targeting the protein to the
508 chloroplast following release from the PM. Remarkably, the Arabidopsis N-myristoylome is
509 enriched in defence-related proteins (Boisson et al., 2003). Our results show that CPK16 localizes
510 to the PM in basal conditions, as previously observed (Stael et al., 2011), but can re-localize to
511 chloroplasts following activation of PTI; chloroplast-localized CPK16 enhances chloroplast-
512 dependent PTI responses, indicating that this protein can act as a modulator of defence through
513 its function in the chloroplast. Many other Arabidopsis proteins containing both targeting signals
514 are known defence regulators (e.g. BIK1, BSK1, AGI1, CPK28); whether these and the other
515 proteins in this subset localize in the chloroplast under specific conditions, and if so, what their
516 function in the organelle and their contribution to defence responses are remains to be
517 investigated. Of note, the subsets of proteins containing these two targeting signals present an
518 over-representation of protein kinases in all species analysed (*C. reinhardtii*, *M. polymorpha*, *P.*
519 *patens*, *A. thaliana*, *O. sativa*, and *S. lycopersicum*), suggesting that kinases that work in other
520 subcellular compartments can function in the chloroplast upon perception of certain stimuli, and
521 underscoring the potential relevance of protein phosphorylation for signalling relay in this putative
522 pathway.

523 Strongly supporting the notion of this pathway having a central function in plant defence is the
524 finding that its co-option and potential disruption by pathogens has evolved multiple times
525 independently: effectors containing an N-myristoylation motif and a cTP and suppressing
526 chloroplast-dependent defences from this organelle have been identified as encoded by DNA
527 viruses, RNA viruses, and bacteria. Future work will unveil how prevalent the coexistence of these
528 two signals is among pathogen effectors, including those belonging to other kingdoms of life.

529 The pathway proposed here would allow for timely, rapid, and precise information relay from the
530 PM to the chloroplast, fine-tuning retrograde signalling to orchestrate appropriate responses upon
531 signal integration in the plastid, avoiding negative consequences of activating defence and
532 shutting down photosynthesis in the absence of a threat. Additionally, it could allow for dual
533 functions of the participating proteins, since they could exert a given role in basal conditions, at
534 the PM, and a different one once a biotic threat is perceived and they are translocated into the
535 chloroplast – for example, by keeping signalling in an off state in the absence of stimulus, but
536 promoting downstream responses upon pathogen perception.

537

538

Figure 6. Model of the proposed pathway linking plasma membrane to chloroplasts and activating defence in plants and its co-option by plant pathogens to promote virulence through suppression of SA responses. On the right, the plant defence regulator CPK16; on the left, pathogen-encoded proteins (CP: CP protein from the cucumovirus *Cucumber mosaic virus* (Fam. *Bromoviridae*); P3: P3 protein from the nepovirus *Grapevine fanleaf virus* (Fam. *Secoviridae*); GALA1: GALA1 effector from *R. solanacearum* GMI1000; C4 (EACMV): C4 protein from the bipartite begomovirus *East African cassava Mosaic virus* (Fam. *Geminiviridae*); C4 (BCTV): C4 protein from the curtovirus *Beet curly top virus* (Fam. *Geminiviridae*); C4 (TYLCV): C4 from the monopartite begomovirus *Tomato yellow leaf curl virus* (Fam. *Geminiviridae*); CAS: Plant-encoded Calcium sensing receptor protein). Activation of defence following perception of a biotic threat at the plasma membrane would trigger release of the indicated proteins and their subsequent re-localization to chloroplasts, where they would activate (green arrow) or repress (red arrows) downstream SA-dependent defence responses.

One example of how the subcellular compartmentalization enabled by protein re-localization can give rise to multifunctionality is illustrated by the C4 protein encoded by TYLCV. At the PM, C4 interacts with the receptor-like kinases BAM1 and BAM2 and hinders the intercellular spread of RNAi (Rosas-Diaz et al., 2018; Fan et al., 2019); following activation of defence, however, which is triggered by the presence or activity of the virus-encoded Rep protein, C4 is translocated to the chloroplast, where it interacts with CAS and interferes with the CAS-dependent defence responses, including SA biosynthesis. Therefore, C4 can exert at least two distinct biological

558   functions depending on its subcellular localization, which is determined by the state of the cell,
559   both of which promote viral pathogenicity. This model could also apply to other pathogen effectors,
560   which could have additional virulence-promoting roles at the PM in the absence of a defensive
561   trigger. The identification of the targets of independently evolved effectors following chloroplast
562   translocation could make a powerful contribution to elucidating the molecular mechanisms
563   involved in chloroplast-nucleus communication during plant-pathogen interactions.

564   In addition to expanding our view of the molecular and cellular underpinnings of plant defence,
565   the unravelling of the direct physical connection between PM and chloroplasts following the
566   perception of a biotic threat could also have practical applicability, paving the way to the
567   engineering of improved resistance to pathogens without yield penalty. This idea is suggested by
568   the results obtained with transgenic CPK16$_{G2A}$ Arabidopsis plants, which show no apparent
569   developmental phenotype, with no effect in growth, but are more resistant to bacterial infection.
570   This observation also implies that chloroplast localization is not sufficient for CPK16 to activate
571   defence responses in the absence of a trigger, and that some additional component, regulated
572   by perception of a biotic threat, is required for the downstream effects.

573   An intriguing question is how these myristoylated, PM-localized proteins get released in order to
574   be translocated to the chloroplast. Since myristoylation is an irreversible covalent lipidation, an
575   additional post-translational modification would be required for the release to occur. In animals,
576   myristoylation-dependent PM association has been shown to be regulated by phosphorylation of
577   the protein (Thelen et al., 1991); since phosphorylation is a prevalent event during activation of
578   defence signalling at the PM, this modification might be a plausible candidate to modulate the
579   localization of plant defence regulators or mimicking pathogen effectors. As the results with the
580   non-myristoylable versions of these plant- or pathogen-encoded proteins indicate, PM release
581   would be sufficient to guarantee immediate chloroplast localization.

582   Multiple environmental and developmental cues are perceived at the PM. Considering their
583   central role in plant biology, it would be conceivable that some of these signals get relayed to
584   chloroplasts in order to coordinate appropriate downstream physiological responses. In this
585   scenario, whether a similar, post-translational modification-based mechanism operates to enable
586   communication between the PM and chloroplasts following perception of non-defence related
587   cues is a question that remains to be explored.

588

589

22

590 **METHODS**

591 **Transient expression in *Nicotiana benthamiana***

592 Transient expression assays were performed as described in Wang et al. (2017a) with minor

593 modifications. In brief, the *Agrobacterium tumefaciens* strain GV3101 harbouring the

594 corresponding binary vectors were liquid cultured in LB with the appropriate antibiotics at 28°C

595 overnight. Bacterial cultures were centrifuged at 4,000 g for 10 min and resuspended in the

596 infiltration buffer (10 mM $MgCl_2$, 10 mM MES pH 5.6, 150 µM acetosyringone) to an OD_{600} = 0.2-

597 1. Bacterial suspensions were incubated at room temperature in the dark for 2 h before infiltration

598 into the abaxial side of 4-week-old *N. benthamiana* leaves with a 1 mL needle-less syringe. For

599 experiments that required co-infiltration, the *Agrobacterium* suspensions carrying different

600 constructs were mixed at 1:1 ratio before infiltration.

601

602 **Chloroplast isolation**

603 Chloroplasts were isolated from 3-week-old Arabidopsis and 4-week-old *N. benthamiana* plants

604 as described previously (Kauss et al., 2012). Isolated chloroplasts were separated into membrane

605 and stroma fractions according to (Wang et al., 2016). During the course of the fractionation,

606 SIGMAFAST^{TM} Protease Inhibitor was added to all required buffers (1 tablet per 300 ml buffer).

607 Chlorophyll from separated membrane fractions was removed using acetone (Wang et al., 2016).

608 The resulting proteins from pellet and stroma fractions were resuspended in 1x Laemmli SDS

609 sample buffer and denatured for 10 min at 95 °C.

610 Equal amounts of the solubilized protein fractions were separated on 10% SDS-PAGE gels and

611 blotted onto PVDF membranes (Bio-Rad). RFP-fused proteins were detected using a rat anti-RFP

612 antibody (1:5,000; ChromoTek). Light harvesting complex protein (LhcB1) and Rubisco large

613 subunit (RbcL) proteins were immunochemically detected using rabbit anti-LhcB1 (1:10,000;

614 Agrisera) and rabbit anti-RbcL (1:10,000; Agrisera) antibodies, respectively.

615 To detect GALA1$_{G2A}$ and GALA3$_{G2A}$, chloroplasts were isolated from 4-week-old *N. benthamiana*

616 plants expressing GALA$_{G2A}$-GFP proteins (2 dpi) as described previously (Kauss et al., 2012).

617 GFP-Trap beads (GFP-Trap Agarose; ChromoTek) were added to the isolated chloroplast

618 proteins. The samples were first agitated at room temperature for 1.5-2 h, then the beads were

619 washed 4 times for 5 min with wash buffer. Finally, the washed beads were resuspended in 100µl

620 1x Laemmli SDS sample buffer and incubated for 20 min at 70 °C. Equal amounts of the eluted

23

621   proteins were separated on 10% SDS-PAGE gels and blotted onto PVDF membranes (Bio-Rad).

622   GFP-fused proteins were detected using mouse monoclonal anti-GFP antibody (1:5,000;

623   Abiocode).

624

Thylakoid membrane isolation and topology analysis

626   Thylakoid membranes were isolated from 4-week-old plants as described by Kato et al. (2018).

627   Leaves were homogenized in a blender with ice-cold homogenization buffer (0.35 M Sucrose, 50

628   mM HEPES pH 7.5, 0.5 mM $MgCl_2$, 10 mM NaCl, and 2 mM EDTA). Homogenates were then

629   filtered through Miracloth (Merck Millipore). After centrifugation at 2,380 $\times g$ for 10 min, the pellet

630   was resuspended in the same buffer. After centrifugation at 300 $\times g$ for 1 min, the supernatant

631   was centrifuged at 2,380 $\times g$ for 10 min. The pellets were resuspended in the homogenization

632   buffer and used for further analyses.

633   For topology analysis, freshly isolated thylakoid membranes were resuspended (0.5 mg

634   chlorophyll/ml) in HS buffer (0.35 M Sucrose, 50 mM HEPES, pH 7.5 mM) and treated with

635   thermolysin (100 µg/ml) for 30 min on ice. The soluble- and pellet-fractions were then separated

636   by centrifugation at 2,380 $\times g$ for 5 min. Chlorophyll from pellet fractions was removed using

637   acetone. The resulting proteins from pellet and soluble fractions were resuspended in 1x Laemmli

638   SDS sample buffer and denatured for 10 min at 95 °C. Equal amounts of the solubilized protein

639   fractions were separated on 10% SDS-PAGE gels and blotted onto PVDF membranes (Bio-Rad).

640   Protochlorophyllide oxidoreductase (POR) and photosystem II subunit O (PsbO) proteins were

641   immunochemically detected using rabbit anti-POR (1:5,000; Agrisera) and rabbit anti-PsbO

642   (1:10,000; Agrisera) antibodies, respectively.

643

Co-immunoprecipitation (co-IP) and western blot

645   To detect the interaction between C4 and CAS, thylakoid membranes were first isolated to extract

646   proteins. Co-immunoprecipitation (co-IP) was carried out as described previously (Dogra et al.,

647   2019; Wang et al., 2016). Briefly, freshly isolated thylakoid membranes were resuspended in co-

648   IP buffer and kept on ice for 20 min followed by centrifugation at 21,000 $\times g$ for 30 min at 4 °C.

649   The supernatant was filtered through a 0.22 µm Millipore Express PES membrane and proteins

650   were quantified using Pierce™ BCA protein assay kit (Thermo Fisher Scientific). Small aliquots

651   were taken as input samples whereas the remaining parts were used for co-IP. RFP-Trap beads

652 (RFP-Trap Agarose; ChromoTek) were added to equal amounts of the co-IP samples. The

653 samples were first agitated at room temperature for 1.5-2 h, then the beads were washed 4 times

654 for 5 min with wash buffer. Finally, the washed beads were resuspended in 100µl 1x Laemmli

655 SDS sample buffer and incubated for 20 min at 70 °C. Equal amounts of the eluted proteins were

656 separated on 10% SDS-PAGE gels and blotted onto PVDF membranes (Bio-Rad). GFP- and

657 RFP-fused proteins were detected using mouse monoclonal anti-GFP antibody (1:5,000;

658 Abiocode) and rat monoclonal anti-RFP antibody (1:5,000; Chromotek), respectively.

659

Calcium burst measurements

661 *N. benthamiana* leaf discs transiently co-expressing aequorin and the construct of interest were

662 floated on Milli-Q water containing 5 µM coelenterazine (Sigma), then kept overnight at 22°C in

663 the dark. A 1 µM solution of the elicitor peptide flg22 was applied to the leaf discs and the transient

664 increase in calcium was immediately recorded. Aequorin luminescence was measured with a

665 NightShade LB 985 In vivo Plant Imaging System (Berthold) equipped with an absolutely light-

666 tight cabinet and a cooled CCD camera; data were analysed with Indigo v2 software.

667

Bacterial infections

669 Three-week-old Arabidopsis plants grown under short-day condition were spray-inoculated with

670 a *Pseudomonas syringae* pv. *tomato* DC3000 inoculum (OD_{600} = 0.2 in 10 mM $MgCl_2$ with 0.02%

671 Silwet L-77) and kept covered for 24 h. Four-week-old Arabidopsis plants grown under short-day

672 condition were infiltrated with a *Pto*DC3000 inoculum (OD_{600} = 0.0002 in 10 mM $MgCl_2$) using a

673 needleless syringe and kept covered for 24 h.

674 Four-week-old *N. benthamiana* leaves were infiltrated with a *P. syringae* pv. *tomato* DC3000

675 *ΔhopQ1-1* suspension (OD_{600} = 0.0002 in 10 mM $MgCl_2$) using a needleless syringe upon

676 transient expression of the construct of interest.

677 Bacterial growth was determined three days after inoculation by plating 1:10 serial dilutions of leaf

678 extracts; plates were incubated at 28 °C for two days before the bacterial cfu were counted.

679

680

681 **Bioinformatic analyses**

682 For the identification of N-myristoylation motifs and chloroplast transit peptides (cTPs) in the
683 predicted proteomes analyzed in this work, detailed information is provided in the Supplemental
684 methods section.

685 In all cases, the N-terminal myristoylation motif and the cTP were predicted by Expasy
686 Myristoylator (https://web.expasy.org/myristoylator/) and ChloroP
687 (http://www.cbs.dtu.dk/services/ChloroP/), respectively.

688 GO term analyses were conducted with topGO
689 (https://bioconductor.org/packages/release/bioc/html/topGO.html); Venn diagrams were drawn
690 by eulerr (https://cran.r-project.org/web/packages/eulerr/index.html).

691

692 **ACKNOWLEDGEMENTS**

705

706 **AUTHOR CONTRIBUTIONS**

707 RL-D conceived the project; LM-P, HT, VD, MW, TR-D, LW, XD, and DZ performed experiments;
708 LM-P, VD, FX, and RL-D analysed data. RL-D wrote the manuscript with input from all authors.

709

710 **DECLARATION OF INTERESTS**

711 The authors declare no competing interests.

712

713 **TABLES**

714 **Table 1.** Identity of the 26 proteins corresponding to 19 unique genes common to the Arabidopsis,

715 tomato, and rice proteomes containing both an N-myristoylation motif and a cTP.

ID	Description
AT1G07570.1	Protein kinase superfamily protein
AT1G07570.2	Protein kinase superfamily protein
AT1G10410.1	Protein of unknown function (DUF1336)
AT1G13970.1	Protein of unknown function (DUF1336)
AT1G14370.1	Protein kinase 2A
AT1G26360.1	Methyl esterase 13
AT1G26970.1	Protein kinase superfamily protein
AT1G59650.1	Protein of unknown function (DUF1336)
AT1G69240.1	Methyl esterase 15
AT2G02800.1	Protein kinase 2B
AT2G02800.2	Protein kinase 2B
AT2G28930.2	Protein kinase 1B
AT2G28930.3	Protein kinase 1B
AT2G41330.1	Glutaredoxin family protein
AT3G02750.1	Protein phosphatase 2C family protein
AT3G02750.2	Protein phosphatase 2C family protein
AT3G20410.1	Calmodulin-domain protein kinase 9
AT3G29770.1	Methyl esterase 11
AT3G57070.1	Glutaredoxin family protein
AT4G23650.1	Calcium-dependent protein kinase 6
AT4G35600.1	Protein kinase superfamily protein
AT4G35600.2	Protein kinase superfamily protein
AT5G02290.1	Protein kinase superfamily protein
AT5G02290.2	Protein kinase superfamily protein
AT5G45290.1	RING/U-box superfamily protein
AT5G45290.2	RING/U-box superfamily protein

716

717

718

REFERENCES

Bhattacharyya, D., and Chakraborty, S. (2018). Chloroplast: the Trojan horse in plant-virus interaction. *Molecular Plant Pathology 19*, 504-518.

Bhattacharyya, D., Gnanasekaran, P., Kumar, R.K., Kushwaha, N.K., Sharma, V.K., Yusuf, M.A., and Chakraborty, S. (2015). A geminivirus betasatellite damages the structural and functional integrity of chloroplasts leading to symptom formation and inhibition of photosynthesis. *Journal of Experimental Botany 66*, 5881-5895.

Boisson, B., Giglione, C., and Meinnel, T. (2003). Unexpected protein families including cell defense components feature in the N-myristoylome of a higher eukaryote. *The Journal of Biological Chemistry 278*, 43418-43429.

Chan, K.X., Phua, S.Y., Crisp, P., McQuinn, R., and Pogson, B.J. (2016). Learning the Languages of the Chloroplast: Retrograde Signaling and Beyond. *Annual Review of Plant Biology 67*, 25-53.

Chen, H., Zhang, Z., Teng, K., Lai, J., Zhang, Y., Huang, Y., Li, Y., Liang, L., Wang, Y., Chu, C.*, et al.* (2010). Up-regulation of LSB1/GDU3 affects geminivirus infection by activating the salicylic acid pathway. *The Plant Journal 62*, 12-23.

Cutolo, E., Parvin, N., Ruge, H., Pirayesh, N., Roustan, V., Weckwerth, W., Teige, M., Grieco, M., Larosa, V., and Vothknecht, U.C. (2019). The High Light Response in Arabidopsis Requires the Calcium Sensor Protein CAS, a Target of STN7- and STN8-Mediated Phosphorylation. *Frontiers in Plant Science 10*, 974.

de Souza, A., Wang, J.Z., and Dehesh, K. (2017). Retrograde Signals: Integrators of Interorganellar Communication and Orchestrators of Plant Development. *Annual Review of Plant Biology 68*, 85-108.

de Torres Zabala, M., Littlejohn, G., Jayaraman, S., Studholme, D., Bailey, T., Lawson, T., Tillich, M., Licht, D., Bolter, B., Delfino, L.*, et al.* (2015). Chloroplasts play a central role in plant defence and are targeted by pathogen effectors. *Nature Plants 1*, 15074.

Ding, X., Jimenez-Gongora, T., Krenz, B., and Lozano-Duran, R. (2019). Chloroplast clustering around the nucleus is a general response to pathogen perception in *Nicotiana benthamiana*. *Molecular Plant Pathology 20*, 1298-1306.

Dogra, V., Li, M., Singh, S., Li, M., and Kim, C. (2019). Oxidative post-translational modification of EXECUTER1 is required for singlet oxygen sensing in plastids. *Nature Communications 10*, 2834.

749 **Exposito-Rodriguez, M.**, Borges, A.A., Borges-Perez, A., and Perez, J.A. (2008). Selection of internal
750   control genes for quantitative real-time RT-PCR studies during tomato development process. *BMC*
751   *Plant Biology 8*, 131.

752 **Fan, P.**, Wang, H., Xue, H., Rosas-Diaz, T., Tang, W., Zhang, H., Xu, L., and Lozano-Duran, R. (2019). The
753   receptor-like kinases BAM1 and BAM2 promote the cell-to-cell movement of miRNA in the root stele
754   to regulate xylem patterning. *bioRxiv*, 603415.

755 **Felix, G.**, Duran, J.D., Volko, S., and Boller, T. (1999). Plants have a sensitive perception system for the
756   most conserved domain of bacterial flagellin. *The Plant Journal 18*, 265-276.

757 **Fondong, V.N.**, Reddy, R.V., Lu, C., Hankoua, B., Felton, C., Czymmek, K., and Achenjang, F. (2007). The
758   consensus N-myristoylation motif of a geminivirus AC4 protein is required for membrane binding and
759   pathogenicity. *Molecular Plant-Microbe Interactions 20*, 380-391.

760 **Gnanasekaran, P.**, Ponnusamy, K., and Chakraborty, S. (2019). A geminivirus betasatellite encoded betaC1
761   protein interacts with PsbP and subverts PsbP-mediated antiviral defence in plants. *Molecular Plant*
762   *Pathology 20*, 943-960.

763 **Gomez-Gomez, L**., and Boller, T. (2000). FLS2: an LRR receptor-like kinase involved in the perception of
764   the bacterial elicitor flagellin in Arabidopsis. *Molecular Cell 5*, 1003-1011.

765 **Jelenska, J.**, van Hal, J.A., and Greenberg, J.T. (2010). *Pseudomonas syringae* hijacks plant stress
766   chaperone machinery for virulence. *Proceedings of the National Academy of Sciences of the United*
767   *States of America 107*, 13177-13182.

768 **Jelenska, J.**, Yao, N., Vinatzer, B.A., Wright, C.M., Brodsky, J.L., and Greenberg, J.T. (2007). A J domain
769   virulence effector of Pseudomonas syringae remodels host chloroplasts and suppresses defenses.
770   *Current Biology 17*, 499-508.

771 **Ji, L.H**., and Ding, S.W. (2001). The suppressor of transgene RNA silencing encoded by Cucumber mosaic
772   virus interferes with salicylic acid-mediated virus resistance. *Molecular Plant-Microbe Interactions*
773   *14*, 715-724.

774 **Jin, X.**, Jiang, Z., Zhang, K., Wang, P., Cao, X., Yue, N., Wang, X., Zhang, X., Li, Y., Li, D.*, et al.* (2018).
775   Three-Dimensional Analysis of Chloroplast Structures Associated with Virus Infection. *Plant*
776   *Physiology 176*, 282-294.

777 **Kachroo, P.**, Yoshioka, K., Shah, J., Dooner, H.K., and Klessig, D.F. (2000). Resistance to turnip crinkle
778   virus in Arabidopsis is regulated by two host genes and is salicylic acid dependent but NPR1,
779   ethylene, and jasmonate independent. *The Plant Cell 12*, 677-690.

780 **Kato, Y.**, and Hyodo, K. (2018). The Photosystem II Repair Cycle Requires FtsH Turnover through the EngA
781   GTPase. *Plant Physiology 178*, 596-611.

782 **Kauss, D.**, Bischof, S., Steiner, S., Apel, K., and Meskauskiene, R. (2012). FLU, a negative feedback
783   regulator of tetrapyrrole biosynthesis, is physically linked to the final steps of the Mg(++)-branch of
784   this pathway. *FEBS Letters 586*, 211-216.

785 **Krenz, B.**, Windeisen, V., Wege, C., Jeske, H., and Kleinow, T. (2010). A plastid-targeted heat shock cognate
786   70kDa protein interacts with the Abutilon mosaic virus movement protein. *Virology 401*, 6-17.

787 **Li, G.**, Froehlich, J.E., Elowsky, C., Msanne, J., Ostosh, A.C., Zhang, C., Awada, T., and Alfano, J.R. (2014).
788   Distinct Pseudomonas type-III effectors use a cleavable transit peptide to target chloroplasts. *The
789   Plant Journal 77*, 310-321.

790 **Li, T.**, Huang, Y., Xu, Z.S., Wang, F., and Xiong, A.S. (2019). Salicylic acid-induced differential resistance to
791   the Tomato yellow leaf curl virus among resistant and susceptible tomato cultivars. *BMC Plant
792   Biology 19*, 173.

793 **Liu, X.Y.**, Yang, J., Xie, L., Li, J., Song, X.J., Chen, J.P., and Zhang, H.M. (2015). P5-2 of rice black-streaked
794   dwarf virus is a non-structural protein targeted to chloroplasts. *Archives of Virology 160*, 1211-1217.

795 **Liu, Y.**, Lan, X., Song, S., Yin, L., Dry, I.B., Qu, J., Xiang, J., and Lu, J. (2018). *In Planta* Functional Analysis
796   and Subcellular Localization of the Oomycete Pathogen Plasmopara viticola Candidate RXLR
797   Effector Repertoire. *Frontiers in Plant Science 9*, 286.

798 **Maimbo, M.**, Ohnishi, K., Hikichi, Y., Yoshioka, H., and Kiba, A. (2007). Induction of a small heat shock
799   protein and its functional roles in Nicotiana plants in the defense response against *Ralstonia
800   solanacearum*. *Plant Physiology 145*, 1588-1599.

801 **Malamy, J.**, Carr, J.P., Klessig, D.F., and Raskin, I. (1990). Salicylic Acid: a likely endogenous signal in the
802   resistance response of tobacco to viral infection. *Science* (New York, NY) *250*, 1002-1004.

803 **Mukaihara, T.**, Tamura, N., and Iwabuchi, M. (2010). Genome-wide identification of a large repertoire of
804   Ralstonia solanacearum type III effector proteins by a new functional screen. *Molecular Plant-
805   Microbe Interactions 23*, 251-262.

806 **Nomura, H.**, Komori, T., Uemura, S., Kanda, Y., Shimotani, K., Nakai, K., Furuichi, T., Takebayashi, K.,
807   Sugimoto, T., Sano, S*., et al.* (2012). Chloroplast-mediated activation of plant immune signalling in
808   Arabidopsis. *Nature Communications 3*, 926.

809 **Park, Y.G.**, Mun, B.G., Kang, S.M., and Hussain, A. (2017). Bacillus aryabhattai SRB02 tolerates oxidative
810   and nitrosative stress and promotes the growth of soybean by modulating the production of
811   phytohormones. *PLOS One 12*, e0173203.

812 **Petre, B.**, Lorrain, C., Saunders, D.G., Win, J., Sklenar, J., Duplessis, S., and Kamoun, S. (2016). Rust fungal
813   effectors mimic host transit peptides to translocate into chloroplasts. *Cellular Microbiology 18*, 453-
814   465.

815 **Qi, G.**, Chen, J., Chang, M., Chen, H., Hall, K., Korin, J., Liu, F., Wang, D., and Fu, Z.Q. (2018).
816   Pandemonium Breaks Out: Disruption of Salicylic Acid-Mediated Defense by Plant Pathogens.
817   *Molecular Plant 11*, 1427-1439.

818 **Rodriguez-Herva, J.J.**, Gonzalez-Melendi, P., Cuartas-Lanza, R., Antunez-Lamas, M., Rio-Alvarez, I., Li,
819   Z., Lopez-Torrejon, G., Diaz, I., Del Pozo, J.C., Chakravarthy, S*., et al.* (2012). A bacterial cysteine
820   protease effector protein interferes with photosynthesis to suppress plant innate immune responses.
821   *Cellular Microbiology 14*, 669-681.

822 **Rosas-Diaz, T.**, Zhang, D., Fan, P., Wang, L., Ding, X., Jiang, Y., Jimenez-Gongora, T., Medina-Puche, L.,
823   Zhao, X., Feng, Z*., et al.* (2018). A virus-targeted plant receptor-like kinase promotes cell-to-cell
824   spread of RNAi. *Proceedings of the National Academy of Sciences of the United States of America
825   115*, 1388-1393.

826 **Sang, Y.**, Wang, Y., Ni, H., Cazale, A.C., She, Y.M., Peeters, N., and Macho, A.P. (2018). The Ralstonia
827   solanacearum type III effector RipAY targets plant redox regulators to suppress immune responses.
828   *Molecular Plant Pathology 19*, 129-142.

829 **Sang, Y.**, Yu, W., Zhuang, H., Wei, Y., Derevnina, L., Luo, J., and Macho, A.P. (2019). Intra-strain elicitation
830   and suppression of plant immunity by *Ralstonia solanacearum* type-III effectors in *Nicotiana
831   benthamiana*. *bioRxiv*, 780890.

832 **Segonzac, C.**, Feike, D., Gimenez-Ibanez, S., Hann, D.R., Zipfel, C., and Rathjen, J.P. (2011). Hierarchy
833   and roles of pathogen-associated molecular pattern-induced responses in *Nicotiana benthamiana*.
834   *Plant Physiology 156*, 687-699.

835 **Serrano, I.**, Audran, C., and Rivas, S. (2016). Chloroplasts at work during plant innate immunity. *Journal of
836   Experimental Botany 67*, 3845-3854.

837 **Stael, S.**, Bayer, R.G., Mehlmer, N., and Teige, M. (2011). Protein N-acylation overrides differing targeting
838   signals. *FEBS Letters 585*, 517-522.

839 **Thelen, M.**, Rosen, A., Nairn, A.C., and Aderem, A. (1991). Regulation by phosphorylation of reversible
840   association of a myristoylated protein kinase C substrate with the plasma membrane. *Nature 351*,
841   320-322.

842 **Vaira, A.M.**, Lim, H.S., Bauchan, G., Gulbronson, C.J., Miozzi, L., Vinals, N., Natilla, A., and Hammond, J.
843   (2018). The interaction of Lolium latent virus major coat protein with ankyrin repeat protein NbANKr

844   redirects it to chloroplasts and modulates virus infection. *The Journal of General Virology 99*, 730-
845   742.

846   **Wang, L.**, Ding, X., Xiao, J., Jimenez-Gongora, T., Liu, R., and Lozano-Duran, R. (2017a). Inference of a
847   Geminivirus-Host Protein-Protein Interaction Network through Affinity Purification and Mass
848   Spectrometry Analysis. *Viruses 9*.

849   **Wang, L.**, Kim, C., Xu, X., Piskurewicz, U., Dogra, V., Singh S., Mahler H., Apel K. (2016). Singlet oxygen-
850   and EXECUTER1-mediated signaling is initiated in grana margins and depends on the protease
851   FtsH2. *Proceedings of the National Academy of Sciences of the United States of America 113*,
852   E3792-3800.

853   **Xiao, Y.**, Wang, J., and Dehesh, K. (2013). Review of stress specific organelles-to-nucleus metabolic signal
854   molecules in plants. *Plant Science 212*, 102-107.

855   **Zhan, B.**, Zhao, W., Li, S., Yang, X., and Zhou, X. (2018). Functional Scanning of Apple Geminivirus Proteins
856   as Symptom Determinants and Suppressors of Posttranscriptional Gene Silencing. *Viruses 10*.

857   **Zhang, Y.**, and Li, X. (2019). Salicylic acid: biosynthesis, perception, and contributions to plant immunity.
858   *Current Opinion in Plant Biology 50*, 29-36.

859   **Zhao, J.**, Zhang, X., Hong, Y., and Liu, Y. (2016). Chloroplast in Plant-Virus Interaction. *Frontiers in*
860   *Microbiology 7*, 1565.

861   **Zhu, J.K.** (2016). Abiotic Stress Signaling and Responses in Plants. *Cell 167*, 313-324.

862

863

864 **SUPPLEMENTAL INFORMATION**

865

866 **SUPPLEMENTAL METHODS**

867

868 **SUPPLEMENTAL FIGURES**

869 **Supplemental figure 1. C4 shifts its localization from the plasma membrane to the**
870 **chloroplast following activation of PTI.**

871 **Supplemental figure 2. C4 interacts with CAS in the chloroplast and suppresses SA-**
872 **dependent defences.**

873 **Supplemental figure 3. Proteins encoded by plant viruses and containing overlapping N-**
874 **myristoylation motifs and cTPs suppress defence responses from the chloroplast.**

875 **Supplemental figure 4. Proteins encoded by the plant pathogenic bacterium *Ralstonia***
876 ***solanacearum* and containing overlapping N-myristoylation motifs and cTPs suppress**
877 **defence responses from the chloroplast.**

878 **Supplemental figure 5. A core of conserved plant defence-related proteins contain**
879 **overlapping N-myristoylation motifs and cTPs.**

880

881 **SUPPLEMENTAL TABLES**

882 **Supplemental table 1.** Identity of the 78 proteins containing both an N-myristoylation motif and
883 a cTP from the Arabidopsis predicted proteome.

884 **Supplemental table 2.** Identity of the 68 proteins containing both an N-myristoylation motif and
885 a cTP from the predicted *Solanum lycopersicum* proteome.

886 **Supplemental table 3.** Identity of the 107 proteins containing both an N-myristoylation motif and
887 a cTP from the predicted *Oryza sativa* subsp. *japonica* proteome.

888 **Supplemental table 4.** Identity of the 19 proteins containing both an N-myristoylation motif and
889 a cTP from the predicted *Chlamydomonas reinhardtii* proteome.

890   **Supplemental table 5.** Identity of the 30 proteins containing both an N-myristoylation motif and

891   a cTP from the predicted *Marchantia polymorpha* proteome.

892   **Supplemental table 6.** Identity of the 21 proteins containing both an N-myristoylation motif and

893   a cTP from the predicted *Physcomitrella patens* proteome.

894   **Supplemental table 7.** Plasmids and constructs used in this work.

895   **Supplemental table 8.** Primers used in this work.

896

897   **SUPPLEMENTAL REFERENCES**

898

899